of this behavior occurred after weaning—just 2% of the 241 informed individuals of known age were first seen lobtail feeding when less than 2 years old—and mothers do not preferentially associate with their offspring after weaning (*14*), which helps explain the lack of maternal influence.

A powerful advantage of the NBDA approach is that it allows the simultaneous consideration of ecological, social, and genetic factors as predictors of individual learning rates, thus moving away from sterile arguments about excluding such factors in the development of behavior and instead reflecting the reality that all behavior develops as an interaction of multiple factors (*1*). Thus, in the present study we are able to describe the roles of both ecology and social transmission in the spread of a feeding innovation, reflecting the notion that social learning allows dynamic adaptation to changing ecological circumstances. Lobtail feeding first appeared in this population during a rapid rise in the abundance of sand lance, which gather in high densities to spawn on Stellwagen Bank, after a crash in another important prey, herring (*18*). Although the purpose of adding a lobtail to the beginning of a bubble-feeding dive sequence is unknown, the link with contemporaneous prey dynamics suggests some function specific to foraging on sand lance, perhaps provoking a tightening of the prey school before bubble entrapment. Our results show that social transmission played a crucial role in the spread of lobtail feeding behavior, which has now persisted over 27 years and multiple generations (*14*). Lobtail feeding can therefore be considered a tradition (*26*), and because humpback populations are known to also carry vocal traditions in the form of song (*10*, *11*), this population can be considered to carry multiple traditions.

References and Notes

1. K. N. Laland, V. M. Janik, *Trends Ecol. Evol.* **21**, 542 (2006).
2. A. Whiten *et al.*, *Nature* **399**, 682 (1999).
3. S. Perry *et al.*, *Curr. Anthropol.* **44**, 241 (2003).
4. C. P. van Schaik *et al.*, *Science* **299**, 102 (2003).
5. M. Krützen, E. P. Willems, C. P. van Schaik, *Curr. Biol.* **21**, 1808 (2011).
6. L. E. Rendell, H. Whitehead, *Behav. Brain Sci.* **24**, 309, discussion 324 (2001).
7. R. L. Kendal *et al.*, *Learn. Behav.* **38**, 220 (2010).
8. A. Whiten, A. Mesoudi, *Philos. Trans. R. Soc. London Ser. B* **363**, 3477 (2008).
9. W. Hoppitt, N. J. Boogert, K. N. Laland, *J. Theor. Biol.* **263**, 544 (2010).
10. M. J. Noad, D. H. Cato, M. M. Bryden, M.-N. Jenner, K. C. S. Jenner, *Nature* **408**, 537 (2000).
11. E. C. Garland *et al.*, *Curr. Biol.* **21**, 687 (2011).
12. D. Wiley *et al.*, *Behaviour* **148**, 575 (2011).
13. J. H. W. Hain, G. R. Carter, S. D. Kraus, C. A. Mayo, H. E. Winn, *Fish Bull.* **80**, 259 (1982).
14. P. Clapham, in *Cetacean Societies: Field Studies of Dolphins and Whales,* J. Mann, R. C. Connor, P. L. Tyack, H. Whitehead, Eds. (Univ. of Chicago Press, Chicago, IL, 2000), pp. 173–196.
15. M. T. Weinrich, M. R. Schilling, C. R. Belt, *Anim. Behav.* **44**, 1059 (1992).
16. S. M. Reader, *Learn. Behav.* **32**, 90 (2004).
17. P. M. Payne *et al.*, *Fish Bull.* **88**, 687 (1990).
18. A. J. Read, *Proc. Biol. Sci.* **268**, 573 (2001).
19. M. Franz, C. L. Nunn, *Proc. Biol. Sci.* **276**, 1829 (2009).
20. W. Hoppitt, K. N. Laland, *Am. J. Primatol.* **73**, 834 (2011).
21. R. Donaldson, H. Finn, L. Bejder, D. Lusseau, M. Calver, *Anim. Conserv.* **15**, 427 (2012).
22. Materials and methods are available as supplementary materials on *Science* Online.
23. C. Ramp, W. Hagen, P. Palsboll, M. Berube, R. Sears, *Behav. Ecol. Sociobiol.* **64**, 1563 (2010).
24. S. J. Cairns, S. J. Schwager, *Anim. Behav.* **35**, 1454 (1987).
25. S. P. Borgatti, *Netdraw Software for Network Visualization* (Analytic Technologies, Lexington, KY, 2002).
26. D. Fragaszy, S. Perry, in *The Biology of Traditions: Models and Evidence,* D. Fragaszy, S. Perry, Eds. (Cambridge Univ. Press, Cambridge, 2003), pp. 1–32.
27. National Marine Fisheries Service (NMFS), National Oceanic and Atmospheric Administration (NOAA), Northeast Fisheries Science Center Bottom Trawl Survey Data. NMFS Ecosystems Survey Branch. Tabular Digital Data: www.iobis.org.

Population Growth in a Wild Bird Is Buffered Against Phenological Mismatch

Thomas E. Reed,[1]* Vidar Grøtan,[2] Stephanie Jenouvrier,[3,4] Bernt-Erik Sæther,[2] Marcel E. Visser[1]

Broad-scale environmental changes are altering patterns of natural selection in the wild, but few empirical studies have quantified the demographic cost of sustained directional selection in response to these changes. We tested whether population growth in a wild bird is negatively affected by climate change–induced phenological mismatch, using almost four decades of individual-level life-history data from a great tit population. In this population, warmer springs have generated a mismatch between the annual breeding time and the seasonal food peak, intensifying directional selection for earlier laying dates. Interannual variation in population mismatch has not, however, affected population growth. We demonstrated a mechanism contributing to this uncoupling, whereby fitness losses associated with mismatch are counteracted by fitness gains due to relaxed competition. These findings imply that natural populations may be able to tolerate considerable maladaptation driven by shifting climatic conditions without undergoing immediate declines.

When environments change over time, individuals with extreme trait values can have higher fitness in the new environment, and thus directional selection toward that end of the phenotype distribution will occur (*1*). Given a heritable basis to trait variation, evolutionary responses may ensue (*2*), but a major concern is that the rate of environmental change might outstrip the pace of evolutionary adaptation, thereby threatening the persistence of populations and species (*3*, *4*). Theoretical models have explored this problem by framing the issue in terms of fitness landscapes, where environmental change causes the fitness optimum to shift through trait space (*4–8*), rendering the population less well-adapted to its environment as compared to the situation before the change. As the lag between mean phenotype and optimum phenotype increases, the strength of directional selection toward the optimum intensifies, but the population is also expected to accrue an increasing "lag load," or demographic cost, in terms of reduced mean fitness (*5–10*). Despite the central importance of these concepts in eco-evolutionary theory and conservation biology (*7*, *11*, *12*), empirical studies quantifying the demographic cost of selection in wild populations are lacking [but see (*13*)].

[1]Department of Animal Ecology, Netherlands Institute of Ecology (NIOO-KNAW), Post Office Box 50, 6700AB Wageningen, Netherlands. [2]Centre for Conservation Biology, Department of Biology, Norwegian University of Science and Technology, NO-7491, Trondheim, Norway. [3]Woods Hole Oceanographic Institution, Woods Hole, MA 02543, USA. [4]Centre d'Etudes Biologiques de Chize, Centre National de la Recherche Scientifique, F-79360 Villiers en Bois, France.

*Corresponding author. E-mail: t.reed@nioo.knaw.nl
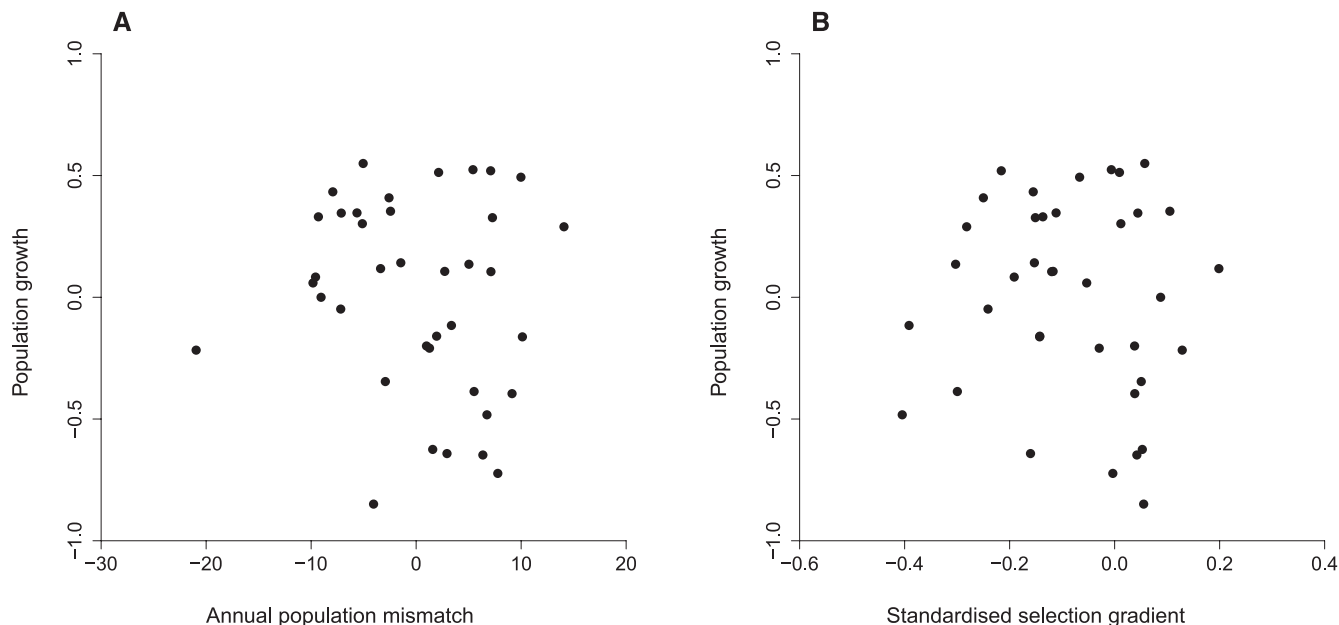
Fig. 1. Population growth as a function of (A) annual population mismatch and (B) annual standardized selection gradient. (A) Positive values on the y axis indicate population increase, negative values indicate population decrease. Positive values on the x axis in- dicate years when mean breeding time is later than the food peak, negative values the opposite. (B) Positive selection gradients indicate selection for later laying dates, negative gradients indicate selection for earlier laying.

Table 1. Results of the GLMM on fitness contributions to population growth ($W_{i,\tau}$). All ex- planatory variables were mean- and variance-standardized before model fitting, hence effect sizes are directly comparable. None of the two-way interactions were significant ($P > 0.05$). A GLMM with Poisson errors and log-link function was used; estimates are on a log scale. Random effects were as follows: female identity variance component = <0.001; year variance component = 0.046. Number of observations = 4177; groups: female identity = 2616; year = 38.

	Estimate	Standard error	z value	Probability (>|z|)
	Significant fixed effects			
Intercept	−0.615	0.044	−14.001	<0.001
Breeding density	−0.220	0.046	−4.738	<0.001
Beech crop	0.185	0.043	4.354	<0.001
Age structure	−0.094	0.044	−2.159	0.031
	Nonsignificant fixed effects			
Population mismatch	−0.054	0.042	−1.260	0.208
Population mismatch^2	0.040	0.032	1.254	0.210
Beech crop^2	−0.032	0.054	−0.585	0.558

Climate change can disrupt preexisting synchrony between interacting species in the seasonal timing (i.e., phenology) of their life-history events (*14*). For example, phenological mismatches between predators and prey are expected to affect both the demography of predator populations (*15*) and selection pressures on traits affecting phenology (*3*), providing an ideal opportunity to characterize the demographic cost of selection. We studied great tits (*Parus major*) in the Netherlands in relation to the phenology of their caterpillar food supply. This part of Western Europe has experienced substantial spring warming in recent decades related to global climate change (*16*). Great tits rely on caterpillars to feed their chicks and strive to match their breeding time with the pronounced seasonal peak in caterpillar biomass,

which enhances offspring survival (*16–19*). Previous studies illustrated how climate change has produced a steadily increasing mismatch between great tit and caterpillar phenology in our study area, because the caterpillar food peak has advanced in response to rising spring temperatures at more than twice the rate of great tit laying dates (*16, 17*). When temperatures during the period after great tits have laid their eggs (late spring) are high, the mismatch is larger (by 2.96 ± 0.43 days per 1°C increase, $F_{1,36} = 47.40$, $P < 0.001$), because caterpillars develop faster under warmer conditions (*19*) and hence the food peak is early relative to the great tit nestling phase. The greater this mismatch, the stronger is directional selection for earlier laying dates (linear regression slope = −0.007 ± 0.003, $F_{1,36} = 5.066$, $P = 0.031$).

If phenological mismatch has detrimental fitness consequences, we expect a negative relationship between annual population growth and population mismatch (*PM*); i.e., reduced population growth in years when breeding is late relative to the food peak. However, there were no statistically significant linear ($F_{1,36} = 0.277$, $P = 0.602$) nor quadratic ($F_{2,35} = 0.179$, $P = 0.602$) effects of *PM* on population growth (Fig. 1A). Moreover, there was no relationship between population growth and directional selection strength (Fig. 1B; linear regression: $F_{1,36} = 0.040$, $P = 0.842$; quadratic regression: $F_{2,35} = 0.956$, $P = 0.394$), implying that mistiming (the deviation between mean laying dates and the moving fitness optimum) did not depress mean fitness. To explore this apparent uncoupling between population growth and *PM* in more detail using individual-level demographic data, we defined a fitness variable $W_{i,\tau} = R_{i,\tau} + S_{i,\tau}$, where $R_{i,\tau}$ was the number of female recruits per breeding female per year and $S_{i,\tau}$ was a binary variable indicating survival to breed again the next year (*20, 21*). We then fitted a generalized linear mixed-effects model (GLMM) (*21*) with $W_{i,\tau}$ as the response variable and used it to test whether interannual variation in absolute fitness (which is strongly positively correlated with population growth, fig. S1) was associated with variation in *PM*. There were no statistically significant linear or quadratic effects of *PM*, even after controlling for the effects of interannual variation in beech nuts [a key winter food source (*20*)], breeding population size, and age structure (Table 1). This confirmed that between-year variation in phenological mismatch did not explain the observed

variation in annual mean fitness and thus did not influence population growth.

These results present a conundrum: Why is population growth not lower in years when a large fraction of females lays too late? There are two reasons. The first is simply that the food peak is typically much narrower than the distribution of laying dates, and hence reproductive fitness cannot be high for all females each year. In years when the mean laying date was early relative to the food peak (negative *PM* years), early females produced fewer fledglings (Fig. 2A) and fewer recruits (Fig. 2B) than late females, whereas intermediate females had the highest reproductive output. In years when mean laying date was relatively late (positive *PM* years), late females had lower reproductive output than intermediate females, who in turn performed more poorly than the earliest females (Fig. 2, A and B). Thus, the overall pattern of fecundity selection has shifted from stabilizing to directional as the population breeds increasingly late relative to the food peak, but average reproductive

output has not been depressed appreciably. The patterns for viability selection (Fig. 2C) are similar, except that in negative *PM* years the latest females have the highest survival, whereas in positive *PM* years they have the lowest survival, potentially because they pay higher energetic costs when provisioning their broods under conditions of food shortage (*22*).

The second reason is that reduced annual fledgling production associated with phenological mismatch (*23*) is counterbalanced by improved post-independence survival of offspring, due to relaxed competition. The survival of juveniles is strongly density-dependent in our study population (*23, 24*); consequently, the total number of new recruits to the breeding population each year is, in fact, unrelated to the number of fledglings produced the previous year (fig. S2). Fewer fledglings in years of strong mismatch, therefore, do not necessarily lead to fewer recruits overall (fig. S2), even though breeding time still determines which females produce the most recruits. Of the two explanations, this latter buffering

mechanism is the most general, because density-dependent compensation (DDC) is a widespread phenomenon in natural populations. For example, sustainable harvesting of wildlife and fish populations is typically based on the premise that increased mortality due to harvest will be partially or fully offset by decreased natural mortality (or increased fecundity) after harvest because of reduced competition for food or territories (*25, 26*). Our proposed mechanism is analogous, except that nestling mortality due to phenological mismatch (rather than harvest) reduces cohort size at the end of the breeding season, which in turn increases per-capita recruitment rates (fig. S2).

The first mechanism implies that if *PM* were to increase further, directional selection would continue to intensify and mean fitness would eventually decrease (in the absence of an evolutionary response). The second mechanism implies, however, that the reduction in mean fitness would be much stronger if not for DDC. To illustrate the interaction between the two mechanisms, we simulated the stochastic population dynamics using
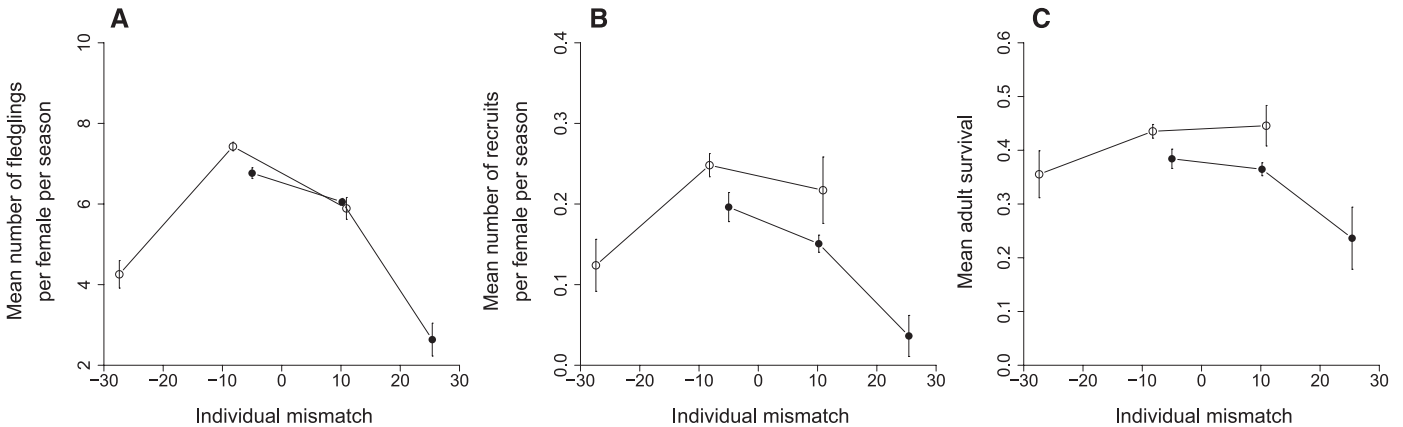
Fig. 2. Fitness components plotted against individual mismatch. (A) Mean number of fledglings, **(B)** mean number of female recruits, and **(C)** mean adult female survival per year plotted against individual mismatch. For illustrative purposes, data were grouped into negative mismatch years ($n = 17$ years, open circles), when the mean breeding time was earlier than the food peak, and positive mismatch years ($n = 21$ years, solid circles), when mean breeding time was later. Data were also binned along the x axis into three equally spaced categories, corresponding to early, intermediate, and late breeders. Error bars are SEM.

Fig. 3. Simulation model results when recruitment was (A) density-dependent and (B) density-independent. Results of the simulation model, in which stochastic population dynamics were projected under a control scenario of no climate change (black = no temporal trend in *PM*) and three scenarios of climate change (blue = mild, red = moderate, and green = strong). In (A), the observed relationship between recruitment and breeding density was used, whereas in (B) the slope of this relationship was set to zero (i.e., density dependence was "turned off").

Shown are median population sizes across 1000 simulations. The small inset graphs show inputted trends in *PM* corresponding to each climate change scenario.
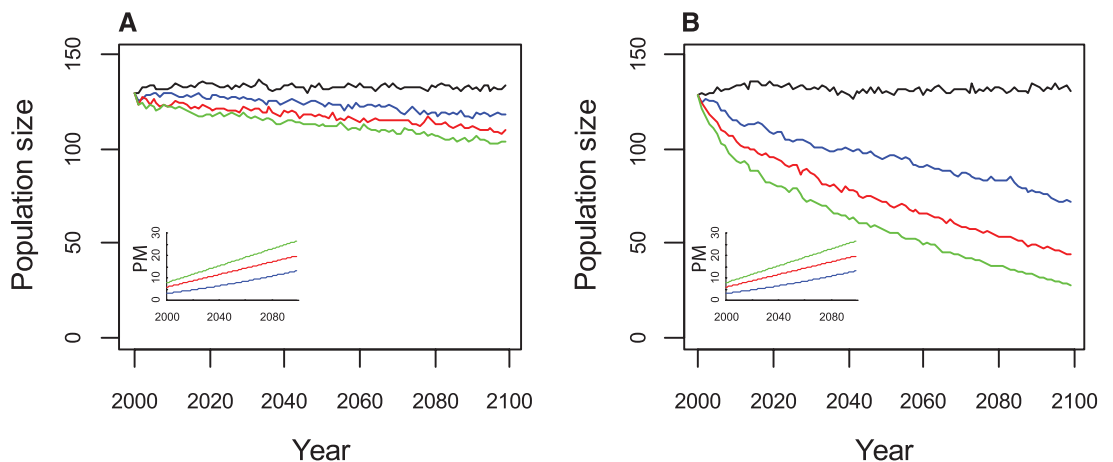
the observed relationships between recruitment/survival and mismatch (21), and projected the population forward in time under the same three scenarios of climate change as described in (27). For each scenario, predicted changes in *PM* were first calculated using output from models of great tit and caterpillar phenology described in (27) and then used as inputs to the current simulation model. The simulations showed that a gradual decline in population size would result if *PM* increases over the next century (assuming no evolutionary response and the same DDC in recruitment rates as observed in the historical data), with the decline being strongest under the most extreme scenario of climate change (Fig. 3A). When DDC in recruitment rates was 'turned off' in the simulations, the rate of population decline for each scenario became substantially stronger (Fig. 3B). This demonstrates that DDC modulates the impacts of mismatch on population growth by partially buffering the population from otherwise more rapid declines.

We found that increasing phenological mismatch driven by climate change had little effect on population growth rates over a study period of almost four decades, despite intensifying directional selection on laying dates. Population numbers therefore remained stable even though late spring temperatures increased by 3.7°C (21). Density dependence within the life cycle partially buffered population growth rate against the negative effects of environmental change, in effect dampening the demographic cost of directional selection. Indeed, theory suggests that the magnitude of the lag load will depend on the form and strength of density regulation, as well as the magnitude of stochastic environmental fluctuations (28). The DDC mechanism we describe here is therefore likely to be of general importance in a wide range of species. For example, Wilson and Arcese (29) found that the population growth of song sparrows was not affected by year-to-year variation in the timing of breeding, despite the latter being strongly correlated with climate. They suggested, but did not demonstrate explicitly, that DDC in recruitment rates could explain this uncoupling. Similar buffering mechanisms might also play a role in dampening the effects of climate change on density-regulated mammal populations, although reductions in mean fitness may be unavoidable when large phenological changes occur (30). Further studies characterizing the lag load in wild populations with different life histories will be crucial to understanding and predicting climate change impacts on population dynamics. Evolutionary adaptation will be critical for persistence in the long run (27), but our results imply that considerable directional selection might be demographically tolerable on decadal time scales without immediate population declines, effectively buying time for microevolution to restore adaptation.

References and Notes

1. J. G. Kingsolver, D. W. Pfennig, *Bioscience* **57**, 561 (2007).
2. D. S. Falconer, T. F. C. Mackay, *Introduction to Quantitative Genetics* (Longmans Green, Harlow, Essex, UK, ed. 4, 1996).
3. M. E. Visser, *Proc. Biol. Sci.* **275**, 649 (2008).
4. L. M. Chevin, R. Lande, G. M. Mace, *PLoS Biol.* **8**, e1000357 (2010).
5. M. Lynch, R. Lande, in *Biotic Interactions and Global Change,* P. M. Kareiva, J. G. Kingsolver, R. B. Huey, Eds. (Sinauer, Sunderland, MA, 1993), pp. 234–250.
6. R. Bürger, M. Lynch, *Evolution* **49**, 151 (1995).
7. J. J. Hellmann, M. Pineda-Krch, *Biol. Conserv.* **137**, 599 (2007).
8. R. Lande, *Evolution* **61**, 1835 (2007).
9. R. Lande, S. Shannon, *Evolution* **50**, 434 (1996).
10. R. Gomulkiewicz, R. D. Holt, *Evolution* **49**, 201 (1995).
11. M. T. Kinnison, N. G. Hairston, *Funct. Ecol.* **21**, 444 (2007).
12. R. Bürger, C. Krall, in *Evolutionary Conservation Biology,* R. Ferriere, U. Dieckmann, D. Couvet, Eds. (Cambridge Univ. Press, Cambridge, 2004), pp. 171–187.
13. N. G. Hairston Jr., S. P. Ellner, M. A. Geber, T. Yoshida, J. A. Fox, *Ecol. Lett.* **8**, 1114 (2005).
14. M. E. Visser, C. Both, *Proc. Biol. Sci.* **272**, 2561 (2005).
15. A. J. Miller-Rushing, T. T. Hoye, D. W. Inouye, E. Post, *Philos. Trans. R. Soc. London Ser. B* **365**, 3177 (2010).
16. M. E. Visser, A. J. van Noordwijk, J. M. Tinbergen, C. M. Lessells, *Proc. R. Soc. London B Biol. Sci.* **265**, 1867 (1998).
17. M. E. Visser, L. J. M. Holleman, P. Gienapp, *Oecologia* **147**, 164 (2006).
18. A. Charmantier et al., *Science* **320**, 800 (2008).
19. A. J. van Noordwijk, R. H. McCleery, C. M. Perrins, *J. Anim. Ecol.* **64**, 451 (1995).
20. V. Grøtan et al., *J. Anim. Ecol.* **78**, 447 (2009).
21. Materials and methods are available as supplementary materials on *Science* Online.
22. D. W. Thomas, J. Blondel, P. Perret, M. M. Lambrechts, J. R. Speakman, *Science* **291**, 2598 (2001).
23. T. E. Reed, S. Jenouvrier, M. E. Visser, *J. Anim. Ecol.* **82**, 131 (2013).
24. C. Both, M. E. Visser, N. Verboven, *Proc. R. Soc. London B Biol. Sci.* **266**, 465 (1999).
25. M. S. Boyce, A. Sinclair, G. C. White, *Oikos* **87**, 419 (1999).
26. K. A. Rose, J. H. Cowan, K. O. Winemiller, R. A. Myers, R. Hilborn, *Fish Fish.* **2**, 293 (2001).
27. P. Gienapp et al., *Philos. Trans. R. Soc. London Ser. B* **368**, 20120289 (2013).
28. R. Lande, S. Engen, B. E. Saether, *Philos. Trans. R. Soc. London Ser. B* **364**, 1511 (2009).
29. S. Wilson, P. Arcese, *Proc. Natl. Acad. Sci. U.S.A.* **100**, 11139 (2003).
30. J. E. Lane, L. E. B. Kruuk, A. Charmantier, J. O. Murie, F. S. Dobson, *Nature* **489**, 554 (2012).
31. A. Gosler, *The Great Tit* (Hamlyn, London, 1993).
32. V. Bauchau, A. Van Noordwijk, *J. Appl. Stat.* **22**, 1031 (1995).
33. H. Schielzeth, *Methods Ecol. Evol.* **1**, 103 (2010).

Simultaneous Femtosecond X-ray Spectroscopy and Diffraction of Photosystem II at Room Temperature

Jan Kern,[1,2] Roberto Alonso-Mori,[2] Rosalie Tran,[1] Johan Hattne,[1] Richard J. Gildea,[1] Nathaniel Echols,[1] Carina Glöckner,[3] Julia Hellmich,[3] Hartawan Laksmono,[4] Raymond G. Sierra,[4] Benedikt Lassalle-Kaiser,[1]* Sergey Koroidov,[5] Alyssa Lampe,[1] Guangye Han,[1] Sheraz Gul,[1] Dörte DiFiore,[3] Despina Milathianaki,[2] Alan R. Fry,[2] Alan Miahnahri,[2] Donald W. Schafer,[2] Marc Messerschmidt,[2] M. Marvin Seibert,[2] Jason E. Koglin,[2] Dimosthenis Sokaras,[6] Tsu-Chien Weng,[6] Jonas Sellberg,[6,7] Matthew J. Latimer,[6] Ralf W. Grosse-Kunstleve,[1] Petrus H. Zwart,[1] William E. White,[2] Pieter Glatzel,[8] Paul D. Adams,[1] Michael J. Bogan,[2,4] Garth J. Williams,[2] Sébastien Boutet,[2] Johannes Messinger,[5] Athina Zouni,[3] Nicholas K. Sauter,[1] Vittal K. Yachandra,[1]† Uwe Bergmann,[2]† Junko Yano[1]†

Intense femtosecond x-ray pulses produced at the Linac Coherent Light Source (LCLS) were used for simultaneous x-ray diffraction (XRD) and x-ray emission spectroscopy (XES) of microcrystals of photosystem II (PS II) at room temperature. This method probes the overall protein structure and the electronic structure of the Mn_4CaO_5 cluster in the oxygen-evolving complex of PS II. XRD data are presented from both the dark state (S_1) and the first illuminated state (S_2) of PS II. Our simultaneous XRD-XES study shows that the PS II crystals are intact during our measurements at the LCLS, not only with respect to the structure of PS II, but also with regard to the electronic structure of the highly radiation-sensitive Mn_4CaO_5 cluster, opening new directions for future dynamics studies.

One of the metalloenzymes most critical for sustaining aerobic life is photosystem II (PS II)—a membrane-bound protein complex found in green plants, algae, and cyanobacteria—that catalyzes the light-driven water oxidation reaction. The oxidation equivalents